Skeletal Radiology (2021) 50:2509–2518
https://doi.org/10.1007/s00256-021-03816-6

SCIENTIFIC ARTICLE

Diagnostic contribution of contrast-enhanced 3D MR imaging of peripheral nerve pathology

Swati Deshmukh[1] · Kyle Tegtmeyer[2] · Mounisha Kovour[3] · Shivani Ahlawat[4] · Jonathan Samet[1]

Received: 8 March 2021 / Revised: 10 May 2021 / Accepted: 10 May 2021 / Published online: 30 May 2021

Abstract

Objective To assess the diagnostic contribution of contrast-enhanced 3D STIR (ce3D-SS) high-resolution magnetic resonance (MR) imaging of peripheral nerve pathology relative to conventional 2D sequences.

Materials and methods In this IRB-approved retrospective study, two radiologists reviewed 60 MR neurography studies with nerve pathology findings. The diagnostic contribution of ce3D-SS imaging was scored on a 4-point Likert scale (1 = no additional information, 2 = supports interpretation, 3 = moderate additional information, and 4 = diagnosis not possible without ce3D-SS). Image quality, nerve visualization, and detection of nerve pathology were also assessed for both standard 2D neurography and ce3D-SS sequences utilizing a 3-point Likert scale. Descriptive statistics are reported.

Results The diagnostic contribution score for ce3D-SS imaging was 2.25 for the brachial plexus, 1.50 for extremities, and 1.75 for the lumbosacral plexus. For brachial plexus, the mean consensus scores for image quality, nerve visualization, and detection of nerve pathology were 2.55, 2.5, and 2.55 for 2D and 2.35, 2.45, and 2.45 for 3D. For extremities, the mean consensus scores for image quality, nerve visualization, and detection of nerve pathology were 2.60, 2.80, and 2.70 for 2D and 1.8, 2.20, and 2.10 for 3D. For lumbosacral plexus, the mean consensus scores for image quality, nerve visualization, and detection of nerve pathology were 2.45, 2.75, and 2.65 for 2D and 2.0, 2.45, and 2.25 for 3D.

Conclusion Overall, our study supports the potential application of ce3D-SS imaging for MRN of the brachial plexus but suggests that 2D MRN protocols are sufficient for MRN of the extremities and lumbosacral plexus.

Keywords MR neurography · Peripheral nerve · Neuropathy · MRI

Introduction

With advances in magnetic resonance (MR) technology, peripheral nerve imaging has become increasingly utilized for evaluation of nerve pathology such as inflammation, nerve injury, and tumors. High-resolution MR imaging of peripheral nerves, also known as MR neurography (MRN), compliments physical exam and electrodiagnostic studies for evaluation of clinically suspected nerve pathology of the brachial plexus, lumbosacral plexus, and extremity nerves. To date, there are no universally accepted practice guidelines for MRN technique. Ideally, MRN is performed on a 3-Tesla (3 T) scanner for superior signal-to-noise ratio and contrast, although lower field strengths can be utilized. Conventional MRN protocols often entail acquisition of multiplanar fluid-sensitive sequences such as fat-suppressed T2-weighted or short tau inversion recovery (STIR) sequences for evaluation of nerve pathology and anatomic or fat-sensitive sequences such as T1 or intermediate weighted images for anatomic assessment [1–5]. Post-contrast T1-weighted fat-suppressed images may be of added value, particularly in patients undergoing MRN for evaluation of masses [6].

While two-dimensional (2D) sequences enable high in-plane spatial resolution, which is necessary to visualize the fascicular architecture of peripheral nerves, the introduction

✉ Swati Deshmukh

Jonathan Samet
jsamet@northwestern.edu

[1] Department of Radiology, Northwestern University Feinberg School of Medicine, 420 E Superior St, Chicago, IL 60611, USA

[2] Northwestern University Feinberg School of Medicine, 420 E Superior St, Chicago, IL 60611, USA

[3] University of Illinois At Urbana-Champaign, 601 E John St, Champaign, IL 61820, USA

[4] Department of Radiology, Johns Hopkins Hospital, 1800 Orleans St, Baltimore, MD 21287, USA

of three-dimensional (3D) techniques to MRN has allowed for isotropic acquisitions that can be reformatted along curved planes to depict the longitudinal course of nerves. 3D turbo spin-echo (TSE) techniques with sampling perfection with application-optimized contrasts using different flip angle evolution (SPACE, Siemens) and complimentary sequences (CUBE, General Electric; VISTA, Philips) create high contrast images that can be reconstructed into maximum intensity projections (MIPs). 3D imaging with multiplanar reconstructions facilitates depiction of nerve anatomy that may be useful for sharing findings with referring clinicians and surgeons. More recently, a contrast-enhanced 3D heavily T2-weighted SPACE-STIR (ce3D-SS) technique has been described which utilizes the T2-shortening effect of gadolinium to suppress vascular and background signal, thereby increasing visibility of nerves. This technique was originally introduced for MRN of the brachial plexus [7, 8].

While various 3D MRN techniques are well-described in the literature, there is limited scientific data regarding the diagnostic contribution of 3D imaging for peripheral nerve pathology relative to conventional 2D MRN imaging [1, 2]. While the ce3D-SS technique has been shown to improve nerve conspicuity and signal-to-noise ratio, it comes at the cost of suppression of background structures such as bones and muscles which may contribute to the interpretation of peripheral nerve pathology. For this reason, ce3D-SS imaging is not a replacement for 2D MRN protocols. Therefore, both the additional time (7–8 min on a 3 T scanner) and the invasive nature of contrast administration required for this technique must be carefully considered. Furthermore, given a cultural trend towards patient-centered care and recent concerns regarding previously unrecognized risks of repetitive gadolinium-based contrast agent exposure, data-driven support for the diagnostic contribution of the ce3D-SS technique is needed [3, 6].

To date, there is no consensus standard for MRN 3D imaging. At our institution, we have over 5 years' experience with ce3D-SS high-resolution MR imaging which is routinely obtained for MRN of the brachial plexus, lumbosacral plexus, and extremities. Our hypothesis was that ce3D-SS imaging is helpful for evaluation of peripheral nerve pathology. The purpose of our study was to retrospectively assess the diagnostic contribution of ce3D-SS high-resolution MRN relative to standard 2D MRN sequences.

Materials and methods

Overview

This HIPAA-compliant IRB-approved study retrospectively reviewed high-resolution MRN imaging at our institution performed for evaluation of suspected neuropathy with the purpose of evaluating the diagnostic contribution of ce3D-SS sequences. Both 2D and contrast-enhanced 3D imaging are routinely obtained at our institution as part of standard neurography protocols.

Subject selection

Our picture archiving communications system (PACS) was searched for all MR neurography studies starting from 12/31/20 and working retrospectively, in order to identify our target goal of 20 MR brachial plexus studies demonstrating nerve pathology (August–December 2020), 20 MR neurography extremity studies demonstrating nerve pathology (November 2019–December 2020), and 20 MR lumbosacral plexus studies demonstrating nerve pathology (December 2018–December 2020). The medical record was reviewed for demographic and correlative clinical data including presenting history, physical exam findings, electrodiagnostic testing, treatment/management decisions, and outcome.

Inclusion criteria were patients aged 18–89 years undergoing standard of care MR neurography at our institution. Exclusion criteria were patients with outside MR neurography imaging, patients with incomplete MR neurography exams or non-neurography MR protocols, and cases where the ce3D-SS technique was not performed (i.e., patient contrast allergy or other contraindication). Patients were excluded if the MR neurography study was interpreted as no evidence of nerve pathology.

MR imaging

MR imaging was performed at our institution in 2018–2020 on a 3-Tesla magnet (Siemens, Erlangen, Germany) or on a 1.5-Tesla magnet (Siemens, Erlangen, Germany) for 5 cases where there was hardware in the area of concern.

2D sequences

For the brachial plexus, we obtain sagittal turbo-spin-echo (TSE) T1-weighted images of the affected side (spinal cord to mid clavicle), sagittal TSE T2-weighted fat-saturated images of the affected side (spinal cord to mid clavicle), coronal TSE T1-weighted images with a small field of view (mid clavicle to mid clavicle), and coronal STIR images with a large field of view (shoulder to shoulder). Our standard MR neurography extremity protocol may vary based on the body part but generally includes multiplanar TSE T2-weighted fat-saturated and T1-weighted images. The MR technologists are asked to clarify the area of interest with the radiologist. Appropriate local array coils are utilized. For the lumbosacral plexus, we utilize a small field of view to cover the lumbar plexus, extending L2 to the greater trochanter, with application of a body phase array coil. The patient is

Table 1 Four-point Likert scale scoring system utilized for assessing diagnostic contribution of contrast enhanced 3D imaging

Score	
1	No additional information
2	Supports interpretation and diagnostic confidence (without adding significant additional information)
3	Adds new information and moderate value to interpretation
4	Essential for accurate interpretation; diagnosis not possible without 3D imaging

asked to empty their bladder prior to the MR exam. The lumbosacral MR protocol entails axial TSE T1-weighted images, coronal TSE T1-weighted images, axial and coronal STIR images, and coronal oblique TSE T1-weighted images through the sacrum. For all neurography studies, pre- and post-contrast 2D T1-weighted fat-saturated images are only obtained if indicated (i.e., for evaluation of neoplasm). All neurography protocols may be adjusted per the radiologist's discretion. Slice thickness is generally 2–3 mm in the coronal plane, 4 mm in the sagittal plane, and 3–4 mm in the axial plane. The time of acquisition is 3–5 min for each 2D scan.

3D sequences

After the administration of intravenous contrast material (Gadavist administered at a dose of 0.1 ml/kg), the ce3D-SS sequence is performed. The ce3D-SS sequence is a heavily T2-weighted SPACE-STIR technique with a slice thickness of 0.8–1.2 mm, typically obtained in the coronal plane. Images are reconstructed into triplanar thin MIPs (5–8 mm thick/1–3 mm spacing). The time of acquisition is 7–8 min for the 3D scan.

Data collection and analysis

The MR imaging was retrospectively reviewed by two board-certified musculoskeletal-subspecialized radiologists with combined 15 years' experience with peripheral nerve imaging. For the purposes of reporting results, discrepancies were resolved by consensus. For each MR exam, the radiologists graded the diagnostic contribution of contrast-enhanced 3D imaging utilizing a 4-point Likert scale (Table 1). The radiologists also graded image quality, visualization of the nerve in question, and visualization of nerve pathology utilizing a 3-point Likert scale for both standard 2D imaging and contrast-enhanced 3D imaging (Table 2). Image quality scoring of 2D images accounted for the success of fat suppression and motion artifact. Image quality scoring of 3D images accounted for the success of background suppression. Data regarding diagnostic contribution was analyzed before and after exclusion of cases with suboptimal 3D image quality and subdivided by clinical indication.

Demographic data (age, gender, clinical symptoms) and body part/nerve in question were reported. Descriptive statistics were performed. Differences in mean diagnostic contribution scores between brachial plexus, extremities, and lumbosacral plexus were assessed with an ANOVA test

Table 2 Three-point Likert scale scoring system utilized for assessing image quality, nerve visualization, and nerve pathology visualization

	1 = Suboptimal	2 = Adequate	3 = Excellent
Image quality 2D	Motion artifact, incomplete fat saturation, metal artifact	Acceptable quality, in line with basic expectation	Outstanding, "textbook" image quality
Nerve visualization 2D	Nerve not well visualized on any sequences	Nerve adequately visualized in at least one plane	Nerve easily visualized, often on all planes
Nerve pathology visualization 2D	Pathology difficult or impossible to visualize	Pathology adequately visualized and characterized in at least one plane	Pathology easily characterized, often on all planes
Image quality 3D	Poor vascular suppression (i.e., < 50%), incomplete fat saturation	Acceptable vascular suppression (i.e., 50–75%)	Complete vascular suppression (i.e., > 75%)
Nerve visualization 3D	Nerve not well visualized	Nerve adequately visualized, at least on the contrast-enhanced coronal 3D T2 SPACE-STIR source sequence	Excellent visualization of nerve, typically on the contrast enhanced coronal 3D T2 SPACE-STIR source and MIPs
Nerve pathology visualization 3D	Pathology difficult or impossible to visualize	Pathology adequately visualized and characterized, at least on one sequence	Excellent visualization of nerve pathology, "textbook" case

with unequal variances. Differences in mean Likert scores between standard 2D imaging and contrast-enhanced 3D images were assessed with a paired Student's t-test, with an $\alpha = 0.05$ significance level.

Results

Our data set included 60 MRN exams (20 brachial plexus, 20 extremities, 20 lumbosacral plexus) with mean age of 48 years (range: 18–76 years) and male:female ratio of 1.3:1. The anatomic region and primary nerves in question are detailed in Table 3. Clinical indication was subdivided into 3 categories: (1) pain, weakness, numbness ($n = 43$); (2) trauma ($n = 7$); and (3) mass ($n = 10$).

Representative examples of diagnostic contribution scores of 1 through 4 are shown in Figs. 1, 2, 3 and 4. There was a significant difference in mean diagnostic contribution scores for the brachial plexus, extremities, and lumbosacral plexus ($p = 0.0388$). For the brachial plexus, the average consensus score for diagnostic contribution of 3D imaging was 2.25, indicating that 3D imaging overall supported 2D interpretation and in some cases contributed moderate additional information facilitating the interpretation of nerve pathology. In all 5 cases where 3D imaging provided no additional information, the 3D image quality was suboptimal (due to failure in vessel and background suppression). For the extremities, the average consensus score for diagnostic contribution of 3D imaging was 1.50, indicating that 3D imaging overall contributed no additional information or supported 2D interpretation. Out of 11 cases where 3D imaging was found to add no additional information, 7 had suboptimal 3D image quality. For the lumbosacral plexus, the average consensus score for diagnostic contribution of 3D imaging was 1.75, indicating that 3D imaging overall supported 2D interpretation or in some cases did not contribute additional information. In 3 of 6 cases where 3D imaging provided no additional information, the 3D image quality was suboptimal. After exclusion of cases with suboptimal 3D image quality (5 brachial plexus cases, 7 extremity cases, 4 lumbosacral plexus cases), the diagnostic contribution scores were 2.67, 1.77, and 1.87 for the brachial plexus, extremities, and lumbosacral plexus, respectively. A summary of average consensus score for the diagnostic contribution of 3D imaging is shown in Table 4, including by clinical indication.

Average consensus score for image quality, nerve visualization, and nerve pathology visualization on 2D and 3D imaging is summarized in Table 5. The average scores for 2D image quality, nerve visualization, and nerve pathology visualization were overall adequate to excellent (2.53, 2.68, and 2.63, respectively). There was only a single case of suboptimal 2D image quality, secondary to patient positioning on an MRN of the brachial plexus. Cases of suboptimal

Table 3 Clinical data — primary nerve in question and anatomic region in our patient cohort

Primary nerve in question	Number of patients	Anatomic Region
Brachial plexus		
Brachial plexus, not otherwise specified	19	–
Suprascapular nerve	1	–
Extremities		
Median	2	Humerus (n = 1) Humerus and forearm (n = 1)
Ulnar	5	Elbow (n = 3) Forearm (n = 2)
Radial	1	Shoulder
Peroneal	3	Knee (n = 2) Femur (n = 1)
Tibial	2	Knee (n = 1) Tibia/fibula (n = 1)
Axillary	1	Shoulder
Long thoracic nerve	1	Shoulder
Sciatic	2	Femur
Multiple	3	Forearm (n = 2) Shoulder (n = 1)
Lumbosacral plexus		
Lumbosacral plexus, not otherwise specified	12	–
Femoral	6	–
Sciatic	2	–

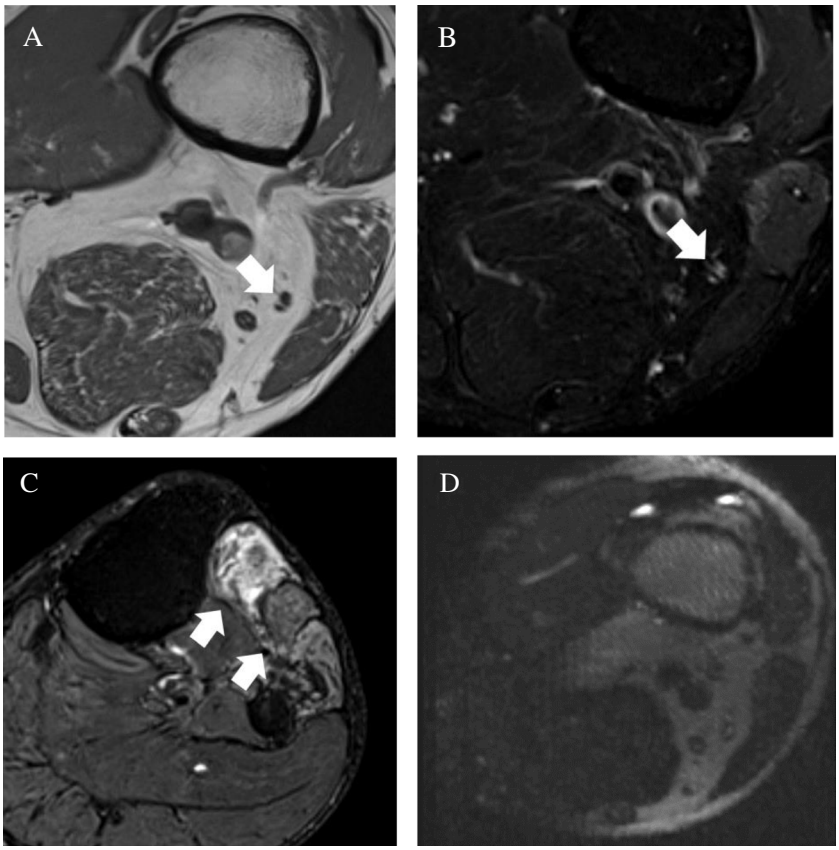

Fig. 1 Sixty-seven-year-old male with foot drop. **A** Axial T1-weighted and **B** STIR images demonstrate signal hyperintensity of the common peroneal nerve (arrow). **C** Distally, axial STIR image demonstrates moderate edema of tibialis anterior and mild edema of extensor digitorum longus and peroneal longus muscles (arrows), compatible with denervation. **D** Axial ce3D-SS MIP is of no added diagnostic value (score of 1) in light of suboptimal image quality

3D image quality were due to failure in vessel and fat suppression. For the brachial plexus, the average scores for 3D image quality, nerve visualization, and nerve pathology visualization were 2.35, 2.45, and 2.45, respectively. For the extremities, the average 3D image quality, nerve visualization, and nerve pathology visualization scores were 1.80, 2.2, and 2.1, respectively. For the lumbosacral plexus, the average 3D image quality, nerve visualization, and nerve pathology visualization scores were 2.0, 2.45, and 2.25.

Discussion

From a technical standpoint, MRN can be challenging due to the small caliber of peripheral nerves and their circuitous course as well as adjacent blood vessels that are similar in size and signal intensity to nerves. Findings of nerve pathology such as signal hyperintensity or fascicular enlargement may also be subtle. For this reason, there has been significant interest in optimizing MRN protocols with 3D and vascular suppression techniques [1, 2, 9]. In this study, we found that ce3D-SS imaging supports interpretation and may contribute additional information for MRN of brachial plexus pathology but was on average of less added diagnostic value for MRN of extremity peripheral nerve and lumbosacral plexus pathology.

The ce3D-SS technique was originally described for imaging of the brachial plexus, as a means of improving visualization of the brachial plexus and its branches relative to 2D MRN and non-contrast-enhanced 3D SPACE-STIR [7, 8]. Non-contrast-enhanced 3D SPACE-STIR imaging of the brachial plexus provides excellent fat suppression and was shown to improve visualization of nerve anatomy and pathology relative to 2D MRN imaging by Viallon et al. in a study of 17 patients (11 with pathology/6 healthy volunteers) [1–5, 10]. Non-contrast-enhanced 3D SPACE-STIR imaging of the brachial plexus can be limited, however, because signal-to-noise ratio decreases at the shoulders and requires thicker slices to adequately cover complex brachial plexus anatomy which increases overlap between nerves and high signal intensity veins [7]. For this reason, the ce3D-SS technique was introduced as a means of improving nerve visualization by increasing contrast between nerves and surrounding tissues [7, 8].

Several prior studies have demonstrated the efficacy of ce3D-SS in suppressing vascular signal and improving visualization of nerves for the brachial plexus [7–9, 11]. In a study of 30 patients (17 with pathology/13 normal), Chen et al. demonstrated improved image quality and diagnostic ability of ce3D-SS imaging of the brachial plexus relative to non-contrast-enhanced 3D imaging [8]. These findings were confirmed in a study of 30 patients (3 with pathology/27

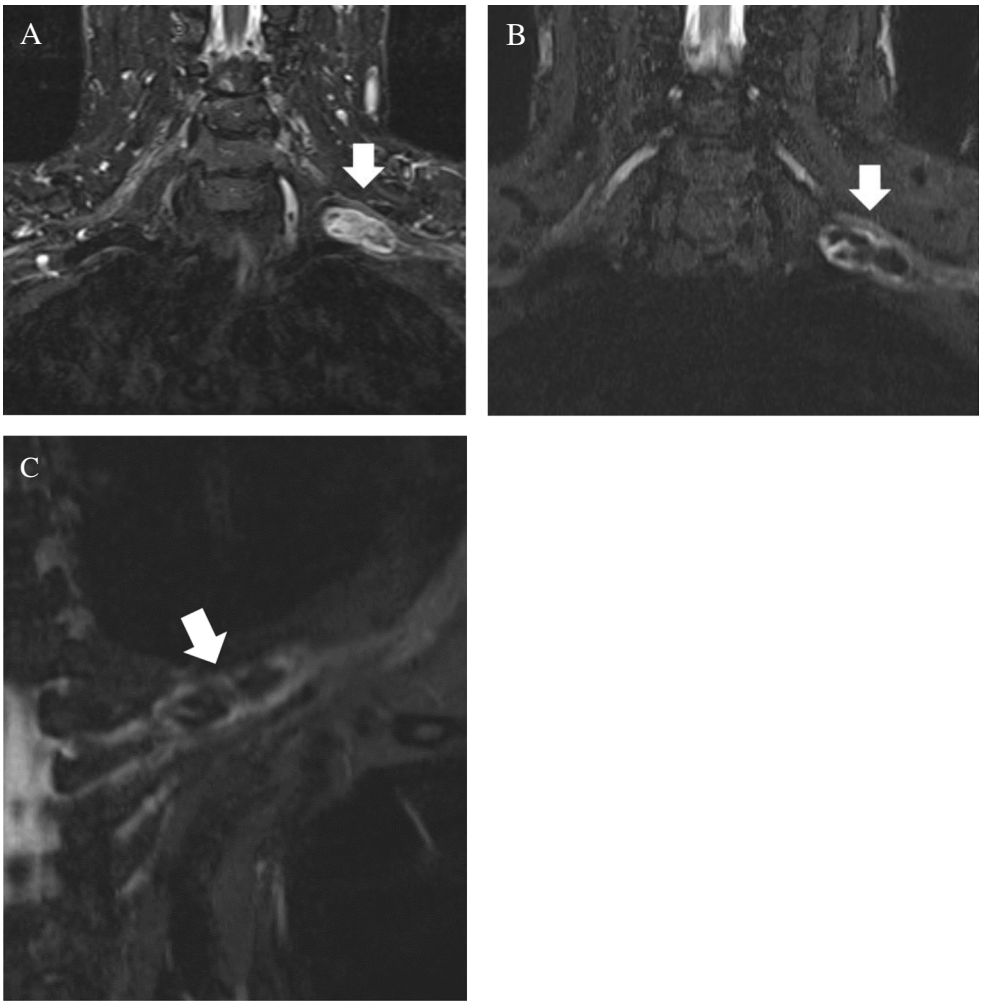

Fig. 2 Sixty-one-year-old male with brachial plexus mass. **A** Coronal STIR image demonstrates a well-circumscribed heterogeneous mass along the left brachial plexus (arrow). 2D image quality, nerve visualization, and nerve pathology visualization were scored as excellent. **B** Coronal ce3D-SS image was also scored as excellent for image quality and visualization of both nerve and nerve pathology. In this case, 3D imaging supported 2D findings (score of 2) without contributing significant additional information. **C** Curved multiplanar reformation, created from 3D sequence, demonstrates the mass (arrow) along the brachial plexus, for demonstration to referring surgeon

normal) by Wang et al. and a study of 27 patients by Xu et al. [7, 11]. In a study of 18 patients (9 with pathology/11 normal), Sneag et al. reported improved visualization of brachial plexus branches (axillary, suprascapular, and musculocutaneous nerves) with contrast-enhanced 3D STIR-FSE relative to non-contrast-enhanced 3D STIR-FSE [9]. Our study supports the technical feasibility of the ce3D-SS technique for brachial plexus MRN. Of note, however, there was no statistically significant difference in image quality, nerve visualization, and nerve pathology visualization between ce3D-SS and 2D imaging of the brachial plexus in our study. This may in part be explained by our institutional experience with MRN allowing for adequate-to-excellent 2D image quality, the predominance of brachial plexus pathology over small branch pathology in our patient cohort, and the experience of the readers.

There is limited prior research regarding the ce3D-SS technique for lumbosacral plexus MRN imaging. In a preliminary study of 24 healthy patients, Zhang Y et al. found improved visualization of the lumbosacral plexus and its branches with ce3D-SS imaging relative to non-contrast-enhanced 3D SPACE-STIR imaging [12]. In a study of the sacral plexus in 40 patients, 20 with endometriosis and 20 healthy controls, Zhang X et al. reported that ce3D-SS imaging visualized nerves and increased diagnostic confidence relative to conventional 2D imaging [13]. Our results support the feasibility of the ce3D-SS technique for lumbosacral plexus MRN but found no statistically significant difference in nerve visualization between 2 and 3D imaging. Furthermore, we found a higher nerve pathology visualization score for 2D imaging relative to 3D imaging of the lumbosacral plexus and a lower diagnostic contribution score for the

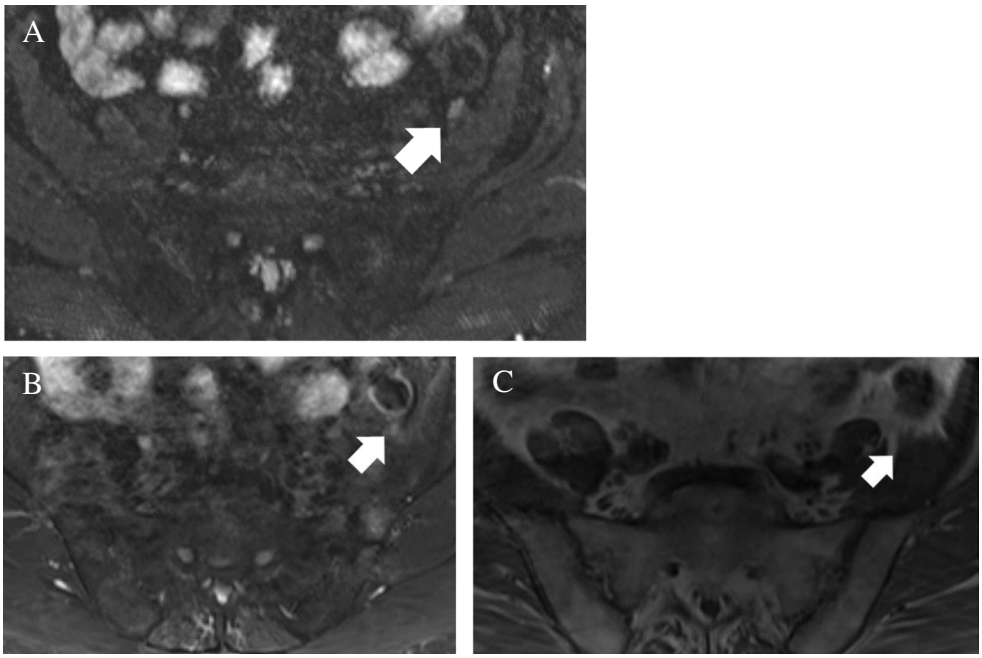

Fig. 3 Fifty-eight-year-old female with suspected left femoral neuropathy after fall. **A** Axial ce3D-SS MIP demonstrates asymmetric enlargement and signal hyperintensity of the left femoral nerve (arrow). While findings can be seen on **B** axial STIR and **C** T1-weighted images, 2D imaging was difficult to interpret due to motion artifact. In these cases, 3D imaging was helpful and scored as 3 for diagnostic contribution

lumbosacral plexus relative to the brachial plexus, which may in part reflect our 2D image quality and the experience of the readers.

To the best of our knowledge, there is no original scientific research to date investigating the ce3D-SS technique for MRN of the extremities. Our study does not support the use of the ce3D-SS technique for MRN of the extremities, which may in part be due to technical challenges with ce3D-SS imaging of the extremities as well as the sufficiency of 2D MRN in the extremities. Based on these results, we conclude that a 2D protocol alone is

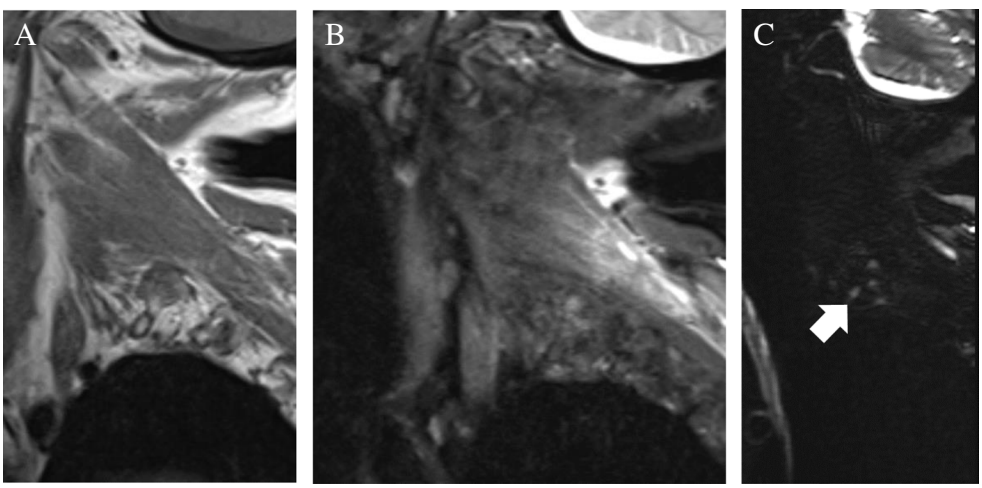

Fig. 4 Seventy-two-year-old female with history of cervical spinal fusion presenting with clinical concern for left brachial traction injury after being found down. **A** Sagittal T1-weighted and **B** T2-weighted fat-saturated images are limited by patient positioning (fixed neck hyperextension) and motion artifact, of suboptimal image quality with poor visualization of nerve pathology. **C** Sagittal ce3D-SS MIP demonstrates signal hyperintensity of the C8 nerve root (arrow). 3D imaging was essential for visualization of the nerves and accurate interpretation of nerve pathology (score of 4)

Table 4 Mean consensus score (grades 1–4) for diagnostic contribution of 3D MR neurography imaging in the total cohort, cohort excluding cases with suboptimal 3D image quality, and total cohort subdivided per clinical presentation

	Total cohort	Adequate or excellent 3D image quality	Pain, weakness, numbness	Trauma	Mass
Brachial plexus	2.25 (n = 20)	2.67 (n = 15)	2.54 (n = 13)	2.00 (n = 3)	1.50 (n = 4)
Extremities	1.50 (n = 20)	1.77 (n = 13)	1.47 (n = 15)	1.67 (n = 3)	1.50 (n = 2)
Lumbosacral plexus	1.75 (n = 20)	1.87 (n = 16)	1.8 (n = 15)	2.00 (n = 1)	1.50 (n = 4)

adequate for MRN of the extremities thereby saving time and contrast agent exposure to the patient.

Alternative 3D techniques that can be utilized for MRN include diffusion-weighted reversed fast imaging with steady-state free precession (3D DW-PSIF) and 3D motion-sensitized driven equilibrium (MDSE). These techniques do not require intravenous contrast. 3D DW-PSIF was shown to improve visualization of nerves relative to 2D T2-weighted imaging in a study of 24 patients undergoing extremity MRN [14] and a second study of 25 healthy patients undergoing extremity, brachial plexus, and lumbosacral plexus MRN [15]. 3D approaches utilizing MDSE for vascular suppression, such as 3D nerve-Sheath signal increased with INKed rest-tissue rarE Imaging (SHINKEI) and modified 3D Nerve View, have also been described as effective for visualizing detailed nerve anatomy [4, 16]. While 3D DW-PSIF and 3D motion-sensitized driven equilibrium techniques are limited by field inhomogeneity susceptibility, long acquisition time, and motion artifact, we hypothesize that they may be advantageous for MRN of the extremities relative to ce3D-SS imaging [1]. Research comparing various 3D MRN techniques is needed.

When subdivided by clinical indication, we found that 3D imaging of the brachial plexus was most helpful for patients presenting with pain, weakness, or numbness; supported 2D imaging interpretation for patients presenting after trauma; and was of less added diagnostic value for patients presenting with mass lesion. Similarly, the average consensus score for diagnostic contribution of 3D imaging of the lumbosacral plexus was less for patients presenting with mass relative to patients presenting with pain, weakness, and numbness. The low number of patients with mass lesions in our brachial plexus (n = 4) and lumbosacral plexus (n = 4) cohorts, however, limits the interpretation of these results. Of note, a prior study by Zhai et al. of 30 patients with peripheral nerve sheath tumors (13 brachial plexus, 9 lumbar plexus, 8 sacral plexus) concluded that ce3D-SS imaging displays the relationship of the tumor to the nerve and improves visualization of nerves relative to non-contrast-enhanced 3D MRN [17]. Further research comparing 3D imaging to 2D neurography for patients with mass lesions is needed.

Limitations of our study include the retrospective design, small sample size, and potential reader bias. Our patient cohort primarily had pathology of larger nerves, which may impact results since 3D MRN offers thinner slices that can be useful for visualization of small nerve branches. In the author's subjective experience, ce3D-SS imaging is valuable for evaluation of very small nerves which may justify the use of intravenous contrast (Fig. 5). Furthermore, we have anecdotally found that ce3D-SS imaging can be helpful when 2D imaging is limited by motion artifact or poor patient positioning; this may not have been reflected in our results given the overall adequate-to-excellent image quality of 2D imaging in our study reflecting institutional familiarity with neurography. Lastly, both readers in this study have experience with peripheral nerve imaging, and hence, the diagnostic contribution of 3D imaging for less experienced readers is not assessed in our study. In particular, the ability to create curved multiplanar reformatted images from 3D imaging may be of added diagnostic value to less experienced readers or radiologists in training. As such, our study did not take into account the potential therapeutic impact of

Table 5 Mean consensus score (grades 1–3) for image quality, nerve visualization, and nerve pathology visualization on 2D and 3D MR neurography imaging

	2D	3D	p-value
Acquisition time (min)	3–5 min per pulse sequence	7–8 min	
Image quality			
Overall (n = 60)	2.53	2.05	**p < 0.001**
Brachial plexus (n = 20)	2.55	2.35	p = 0.385
Extremities (n = 20)	2.60	1.80	**p = 0.001**
LS plexus (n = 20)	2.45	2.00	**p = 0.004**
Nerve visualization			
Overall (n = 60)	2.68	2.36	**p = 0.007**
Brachial plexus (n = 20)	2.50	2.45	p = 0.825
Extremities (n = 20)	2.80	2.20	**p = 0.004**
LS plexus (n = 20)	2.75	2.45	p = 0.083
Nerve pathology visualization			
Overall (n = 60)	2.63	2.27	**p = 0.001**
Brachial plexus (n = 20)	2.55	2.45	p = 0.577
Extremities (n = 20)	2.70	2.10	**p = 0.010**
LS plexus (n = 20)	2.65	2.25	**p = 0.028**

Bold indicates statistical significance

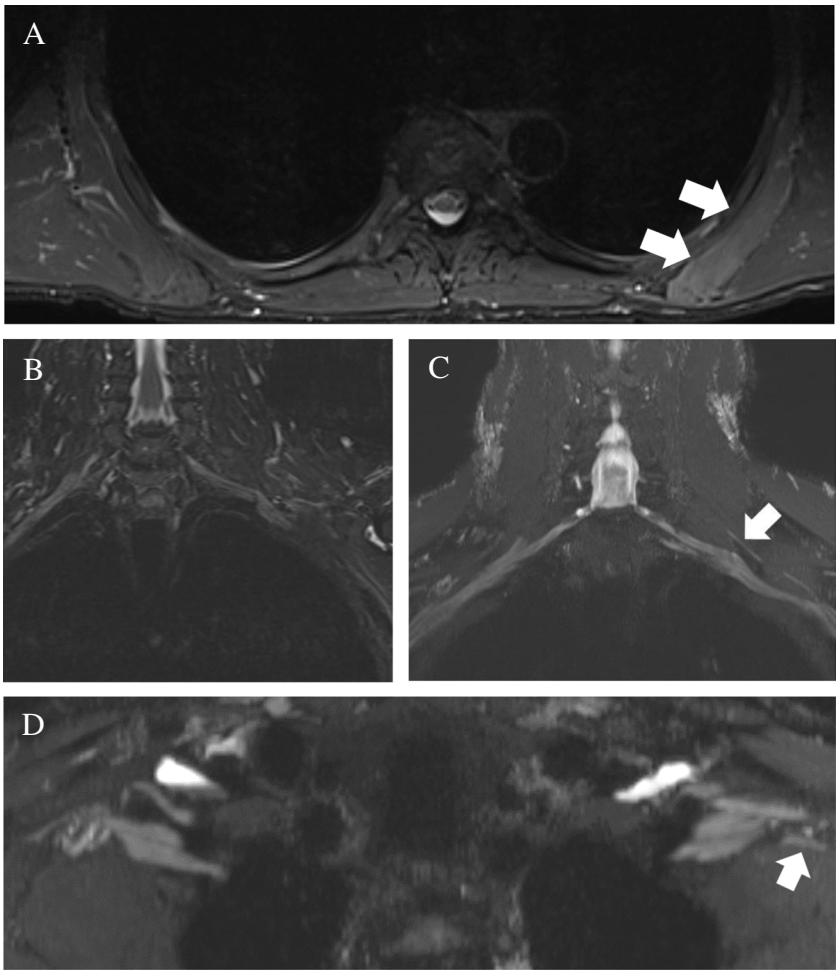

Fig. 5 Fifty-seven-year-old male* with acute-onset left shoulder pain and new winged scapula following surgery for left carpal tunnel release. Electrodiagnostic studies found mild serratus anterior muscle denervation. **A** Axial STIR image demonstrates mild asymmetric edema of the left serratus anterior muscle (arrow) compatible with mild denervation. **B** Coronal STIR image of the brachial plexus adequately demonstrates the brachial plexus itself, but the long thoracic nerve is difficult to identify. **C,D** Coronal and axial ce3D-SS MIPs readily demonstrate the left long thoracic nerve (arrow), which is asymmetrically hyperintense, as it pierces the middle scalene muscle and courses superficial to the serratus anterior muscle. Findings were favored to represent Parsonage-Turner syndrome. *Patient not included in study cohort due to date range

3D imaging for sharing findings with referring clinicians and surgeons.

Conclusion

In the era of patient-centered practice, data-driven optimization of MRI protocols with consideration of both patient comfort and diagnostic performance is important. While the recent development of various 3D techniques has certainly advanced the field of peripheral nerve imaging, new questions arise regarding the necessity, individual drawbacks, and benefit-to-risk ratio of each technique particularly if intravenous contrast is required. Our study supports the potential application of ce3D-SS imaging for MRN of the brachial plexus but suggests that 2D MRN protocols are sufficient for MRN of the extremities and lumbosacral plexus. Further research on the diagnostic contribution of non-contrast 3D SPACE STIR imaging is needed. Data-driven parameters for 2D and 3D MRN protocols throughout the body are needed to develop consensus-based practice guidelines.

Declarations

Conflict of interest The authors declare no competing interests.

References

1. Sneag DB, Queler S. Technological advancements in magnetic resonance neurography. Curr Neurol Neurosci Rep. 2019;19(10):75. https://doi.org/10.1007/s11910-019-0996-x.
2. Chhabra A, Thawait GK, Soldatos T, Thakkar RS, Del Grande F, Chalian M, Carrino JA. High-resolution 3T MR neurography of the brachial plexus and its branches, with emphasis on 3D imaging. AJNR Am J Neuroradiol. 2013;34(3):486–97. https://doi.org/10.3174/ajnr.A3287.
3. Chhabra A, Rozen S, Scott K. Three-dimensional MR neurography of the lumbosacral plexus. Semin Musculoskelet Radiol. 2015;19(2):149–59. https://doi.org/10.1055/s-0035-1545077.
4. Mazal AT, Faramarzalian A, Samet JD, Gill K, Cheng J, Chhabra A. MR neurography of the brachial plexus in adult and pediatric age groups: evolution, recent advances, and future directions. Expert Rev Med Devices. 2020;17(2):111–22. https://doi.org/10.1080/17434440.2020.1719830.
5. Chhabra A. Peripheral MR neurography: approach to interpretation. Neuroimaging Clin N Am. 2014;24(1):79–89. https://doi.org/10.1016/j.nic.2013.03.033.

6. Harrell AD, Johnson D, Samet J, Omar IM, Deshmukh S. With or without? A retrospective analysis of intravenous contrast utility in magnetic resonance neurography. Skeletal Radiol. 2020;49(4):577–84. https://doi.org/10.1007/s00256-019-03321-x.
7. Wang L, Niu Y, Kong X, Yu Q, Kong X, Lv Y, Shi H, Li C, Wu W, Wang B, Liu D. The application of paramagnetic contrast-based T2 effect to 3D heavily T2W high-resolution MR imaging of the brachial plexus and its branches. Eur J Radiol. 2016;85(3):578–84. https://doi.org/10.1016/j.ejrad.2015.12.001.
8. Chen WC, Tsai YH, Weng HH, Wang SC, Liu HL, Peng SL, Chen CF. Value of enhancement technique in 3D–T2-STIR images of the brachial plexus. J Comput Assist Tomogr. 2014;38(3):335–9. https://doi.org/10.1097/RCT.0000000000000061.
9. Sneag DB, Daniels SP, Geannette C, Queler SC, Lin BQ, de Silva C, Tan ET. Post-contrast 3D inversion recovery magnetic resonance neurography for evaluation of branch nerves of the brachial plexus. Eur J Radiol. 2020;132:109304. https://doi.org/10.1016/j.ejrad.2020.109304.
10. Viallon M, Vargas MI, Jlassi H, Lövblad KO, Delavelle J. High-resolution and functional magnetic resonance imaging of the brachial plexus using an isotropic 3D T2 STIR (Short Term Inversion Recovery) SPACE sequence and diffusion tensor imaging. Eur Radiol. 2008;18(5):1018–23. https://doi.org/10.1007/s00330-007-0834-4.
11. Xu Z, Zhang T, Chen J, Liu Z, Wang T, Hu Y, Zhang J, Xue F. Combine contrast-enhanced 3D T2-weighted short inversion time inversion recovery MR neurography with MR angiography at 1.5 T in the assessment of brachial plexopathy. MAGMA. 2020. https://doi.org/10.1007/s10334-020-00867-z.
12. Zhang Y, Kong X, Zhao Q, Liu X, Gu Y, Xu L. Enhanced MR neurography of the lumbosacral plexus with robust vascular suppression and improved delineation of its small branches. Eur J Radiol. 2020;129:109128. https://doi.org/10.1016/j.ejrad.2020.109128.
13. Zhang X, Li M, Guan J, Wang H, Li S, Guo Y, Liu M. Evaluation of the sacral nerve plexus in pelvic endometriosis by three-dimensional MR neurography. J Magn Reson Imaging. 2017;45(4):1225–31. https://doi.org/10.1002/jmri.25435.
14. Chhabra A, Soldatos T, Subhawong TK, Machado AJ, Thawait SK, Wang KC, Padua A Jr, Flammang AJ, Williams EH, Carrino JA. The application of three-dimensional diffusion-weighted PSIF technique in peripheral nerve imaging of the distal extremities. J Magn Reson Imaging. 2011;34(4):962–7. https://doi.org/10.1002/jmri.22684.
15. Zare M, Faeghi F, Hosseini A, Ardekani MS, Heidari MH, Zarei E. Comparison between three-dimensional diffusion-weighted PSIF technique and routine imaging sequences in evaluation of peripheral nerves in healthy people. Basic Clin Neurosci. 2018;9(1):65–71. https://doi.org/10.29252/NIRP.BCN.9.1.65.
16. De Paepe KN, Higgins DM, Ball I, Morgan VA, Barton DP, deSouza NM. Visualizing the autonomic and somatic innervation of the female pelvis with 3D MR neurography: a feasibility study. Acta Radiol. 2020;61(12):1668–76. https://doi.org/10.1177/0284185120909337.
17. Zhai H, Lv Y, Kong X, Liu X, Liu D. Magnetic resonance neurography appearance and diagnostic evaluation of peripheral nerve sheath tumors. Sci Rep. 2019;9(1):6939. https://doi.org/10.1038/s41598-019-43450-w.